Short communication

Thin-film silica sol–gel coatings for neural microelectrodes

Andrew L. Pierce[a], Salah Sommakia[a], Jenna L. Rickus[a,b], Kevin J. Otto[a,c,*]

[a] The Weldon School of Biomedical Engineering, Purdue University, West Lafayette, IN 47907-1791, United States
[b] School of Agricultural and Biological Engineering, Purdue University, West Lafayette, IN 47907-1791, United States
[c] Department of Biological Sciences, Purdue University, West Lafayette, IN 47907-1791, United States

ARTICLE INFO

ABSTRACT

The reactive tissue response of the brain to chronically implanted materials remains a formidable obstacle to stable recording from implanted microelectrodes. One approach to mitigate this response is to apply a bioactive coating in the form of an ultra-porous silica sol–gel, which can be engineered to improve biocompatibility and to enable local drug delivery. The first step in establishing the feasibility of such a coating is to investigate the effects of the coating on electrode properties. In this paper, we describe a method to apply a thin-film silica sol–gel coating to silicon-based microelectrodes, and discuss the resultant changes in the electrode properties. Fluorescently labeled coatings were used to confirm coating adherence to the electrode. Cyclic voltammetry and impedance spectroscopy were used to evaluate electrical property changes. The silica sol–gel was found to successfully adhere to the electrodes as a thin coating. The voltammograms revealed a slight increase in charge carrying capacity of the electrodes following coating. Impedance spectrograms showed a mild increase in impedance at high frequencies but a more pronounced decrease in impedance at mid to low frequencies. These results demonstrate the feasibility of applying silica sol–gel coatings to silicon-based microelectrodes and are encouraging for the continued investigation of their use in mitigating the reactive tissue response.

© 2009 Elsevier B.V. All rights reserved.

1. Introduction

Obtaining stable chronic recordings of the electrical activity of neurons in the cerebral cortex remains a challenge. The ability to obtain such recordings for an extended period of time through penetrating microelectrodes would facilitate advancement in the understanding of brain physiology and the development of therapies for conditions such as paralysis and epilepsy. One barrier to achieving high quality recordings is the reactive response of cortical tissue to chronically implanted microelectrodes. Over the course of days and weeks following implantation, a sheath of activated glia forms around the electrode, isolating the implanted device from the neuronal tissue (Szarowski et al., 2003). Studies have reported a 'kill zone' around implanted devices in which neuronal cell bodies and fibers become severely reduced in density up to 200 μm around the implantation site (Biran et al., 2005). The reactive tissue response includes both an acute phase, caused by implantation injury, and a chronic response of the tissue to the implanted material itself (Polikov et al., 2005). The tissue response results in a decline in availability of viable neurons for recording, and a reduction in sig-nal to noise ratio over time, which reduces or eliminates the ability to effectively collect recordings (Vetter et al., 2004).

Several techniques have been attempted in order to mitigate the response of cortical tissue to implanted microelectrodes. The application of DC voltages to microelectrodes in the cortex has been shown to temporarily increase signal to noise ratio (SNR) and revive the ability to record from viable neurons (Johnson et al., 2005; Otto et al., 2006). Anti-inflammatory drugs such as dexamethasone (DEX) have been used locally and systemically to try to reduce activation of astrocytes and microglia at the implantation site (Kim and Martin, 2006; Spataro et al., 2005; Wadhwa et al., 2006; Zhong and Bellamkonda, 2007). One group etched the surface of electrodes, creating nano-scale surface features, in order to increase neuronal cell adhesion, and thus increase longevity of recording (Moxon et al., 2004, 2007). Several researchers have applied polymer coatings to electrodes in order to alter the material presented to the tissue. Conductive polymers have been applied to silicon-substrate microelectrodes probes to decrease site impedance (Cui et al., 2001; Cui and Martin, 2003; Kim et al., 2004; Ludwig et al., 2006) and laminin coatings have been applied to try to limit tissue reaction (He et al., 2006). More recently, nanotubes formed from conductive polymers have been applied to electrode sites, both reducing site impedance and providing a platform for controlled drug release (Abidian et al., 2006; Abidian and Martin, 2008). Although many of these methods are promising, none have emerged as a definitive solution to the problem of reactive tissue response.

* Corresponding author at: 206 S. Martin Jischke Dr., West Lafayette, IN 47907, United States. Tel.: +1 765 496 1012; fax: +1 765 496 1912.
E-mail addresses: pierce1@purdue.edu (A.L. Pierce), kotto@purdue.edu (K.J. Otto).

One promising new approach to mitigating the reactive tissue response is to coat the microelectrodes in a silica sol–gel. The sol–gel technique allows for application of thin films of ultra-porous silica whose morphology is characterized as a flat surface with pore size and surface features of <25 nm (Jedlicka et al., 2005). The films have a thickness of approximately 100 nm. These ultra-porous sol–gel thin films have been shown to be excellent substrates for neuronal growth (Jedlicka et al., 2006, 2007a). Jedlicka et al. demonstrated that thin films derived from tetramethoxysilane (TMOS)-based sol–gels encourage adhesion of neuronal cells and differentiation of PC12 cells and pluripotent embryonic carcinoma cells into a neuronal phenotype with enhanced neurite outgrowth (Jedlicka et al., 2005, 2006, 2007a). In addition, the application of a TMOS sol–gel coating to microelectrodes may improve biocompatibility by facilitating surface modifications by anchoring biomolecules to the precursor silanes (Jedlicka et al., 2007a,b), which are used in preparation of the gels, or through the controlled release of drugs encapsulated in the porous material (Radin et al., 2005; Radin and Ducheyne, 2007; Santos et al., 1999). This coating technique combines improved material biocompatibility with local drug delivery, and therefore represents a combination of previously attempted techniques for mitigating the reactive tissue response.

Before attempting a chronic *in vivo* biocompatibility experiment, it is necessary to establish the effects of thin-film sol–gel coatings on the electrical properties of the microelectrodes. The purpose of this study is to explore the feasibility of applying thin-film, silica sol–gel coatings to silicon-based microelectrodes. Determining this feasibility includes verifying the adhesion of the coating to the probes, as well as ensuring that the coatings do not significantly detriment the electrode's electrical properties. This characterization is a requisite step toward developing these coatings for the mitigation of the reactive tissue response in order to facilitate chronic recording from the cerebral cortex. The successful mitigation of this response would have wide implications in the study of neurophysiology and the development of neuroprostheses.

2. Materials and methods

2.1. Coating technique

The technique for preparation of thin film sol–gels was previously described (Jedlicka et al., 2006). Briefly, the precursor sol was prepared by mixing 3.8 mL tetramethoxysilane (TMOS) with 850 mL ddH$_2$O, and subsequently adding 0.55 mL of 0.04N HCl to catalyze hydrolysis. The precursor was then sonicated for approximately 15 min. The sonicated mixture was filtered using a 0.2 mm Whatman syringe filter. A solution was then mixed consisting of 300 µL of the filtered TMOS mixture, 700 µL of sterile-filtered, pH 6.0, 0.2 M phosphate buffer, and 100 µL of methanol. The thin films were produced by dip coating the shanks of six single-shank silicon-substrate microelectrodes (NeuroNexus Technologies, Ann Arbor, MI) at a constant rate of 35 mm/s into this final solution. Each of the six electrodes evaluated in this study had 16 individual iridium sites with a site area of 703 µm^2, for a total of 96 coated electrode sites. The films were allowed to gel for approximately 1 min in air at room temperature, and then stored in phosphate buffer for use.

2.2. Evaluation of coating

Sol–gel presence and uniformity on the probes were assessed by the creation of a fluorescently labeled coating. This coating was prepared by adding a saturating quantity of fluorescein sodium salt to the phosphate buffer before coating, resulting in a sol–gel with uniform fluorescent label throughout. A probe was coated in non-fluorescent sol–gel as a control to ensure that the coating itself did not auto-fluoresce. To ensure that fluorescence of the labeled probe was not due to surface adhesion of the fluorescein, coated and uncoated control probes were subsequently dipped in a fluorescein sodium salt solution identical to that used to coat the fluorescent probe, with the exception that the TMOS was replaced with an equal volume of phosphate buffer to forego gelation. Fluorescence micrographs were obtained 1 h after coating using a Leica DM-IRB fluorescence microscope. Images of the fluorescently labeled probes were collected at a 525 nm wavelength emission using 490 nm excitation. The presence of fluorescence in images of the coated probes with fluorescein label was compared against the control probes, which were not labeled.

To evaluate stability of the coating, an established agarose brain model was utilized (Chen et al., 2004). A single shank, acute Michigan probe was coated in the fluorescently labeled sol–gel and imaged as described above. The probe was then inserted repeatedly into the brain model and then imaged again. Stability was assessed by continued fluorescence following insertion in the model.

2.3. Electrical characterization

Electrochemical impedance spectroscopy (EIS) and cyclic voltammetry (CV) measurements were collected using an Autolab potentiostat PGSTAT12 (EcoChemie, Utrecht, The Netherlands) with built in frequency analyzer (Brinkman, Westbury, NY). A three electrode setup was utilized for *in vitro* experiments, with the coated NeuroNexus acute, single-shank electrodes serving as the working electrode. A calomel electrode (Fisher Scientific, Waltham, MA) was used as a reference electrode, and a platinum wire as the counter electrode. Measurements were performed in 1× PBS at room temperature. EIS and CV were preformed prior to and 1 day following application of the thin film coatings. To perform EIS, a 25-mV RMS sine wave was applied to electrode sites with frequencies ranging logarithmically from 0.1 to 10 kHz. CV was performed by sweeping a voltage linearly from −0.6 to +0.8 V at a scanning rate of 1 V/s. Sites with broken or poor connections, detected by having a maximum current in cyclic voltammagrams below 1 nA, were excluded from the data set. The impedance data gathered from EIS were averaged across all sites. The impedances were separated into resistive and reactive components, and were compared for the pre-coated and post-coated probes at all measured frequencies. Changes in resistance, reactance, and impedance magnitude were evaluated using t-tests with $p < 0.05$ indicating significance. Current values from cyclic voltammograms were likewise averaged across all electrode sites. The charge carrying capacity was calculated by integrating the cathodic current density curve generated by the cyclic voltammogram and dividing by the sweep rate, and was compared before and after coating.

3. Results

Fluorescence micrographs revealed the presence of the fluorescent marker on the electrode coated with the labeled sol–gel but not on the control (Fig. 1). The presence of this marker indicates that the sol–gel was able to successfully adhere to the microelectrode. The majority of the coating labeled as a thin, even coating; however, there were punctate regions of increased fluorescence, indicative of local coating irregularities or clumps of the fluorescein label. Absence of fluorescence on the control probe confirms that the coating is not auto-fluorescent, and that the fluorescence of the labeled probe is not due to surface adhesion of the fluorescent label to the coating, but rather due to encapsulation within the coating. In addition, no fluorescence was observed on an uncoated control probe which was dipped in the fluorescein solution (data not shown), indicating that the fluorescence seen in the experimen-
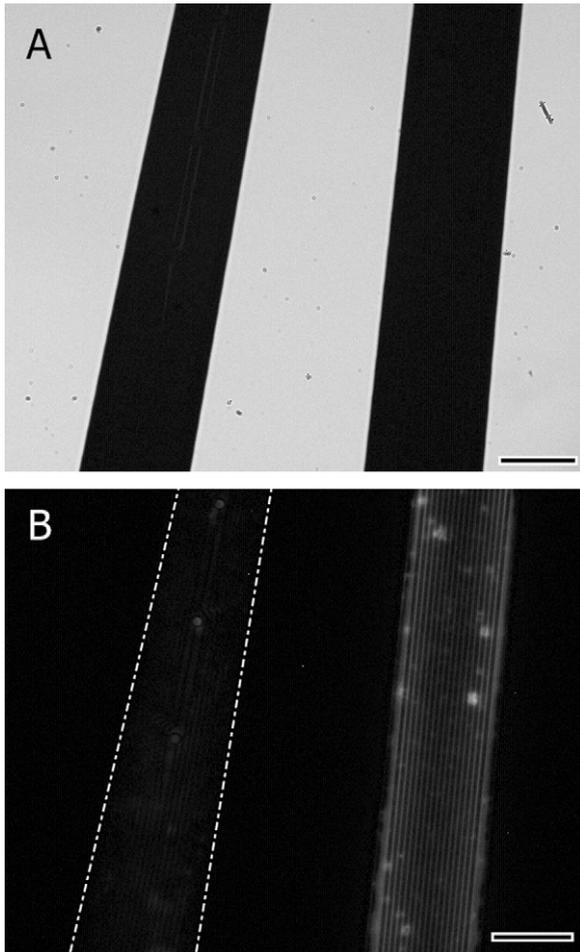
Fig. 1. Microscopy confirms the adherence of sol–gel coatings to microelectrodes. (A) Bright field image of probes to show their location. (B) Fluorescent micrograph of coated probes. For the right probe, fluorescein salt was added to the precursor sol and was encapsulated throughout the coating. The left probe was coated in an unlabeled sol–gel as a control. The unlabeled probe was outlined to demonstrate its location. The fluorescence of the right probe confirms coating adhesion. The absence of fluorescence in the left probe confirms that the coating is not autofluorescent. These images demonstrate that the silica sol–gels can be successfully applied to silicon-based microelectrodes. Additionally, these images confirm the ability to encapsulate molecules in the TMOS precursor to facilitate biomolecule delivery to the implantation site.

Fig. 2. (A) Representitive cyclic voltammogram demonstrates changes in hysteresis curve. Cyclic voltammagrams before and after coating reveal a general increase in current for each applied voltage of the sweep. This result indicates an increase in charge carrying capacity of the electrode site after application of the coating. (B) The average cathodic charge storage capcity ($n = 92$) increases after coating for all experimental sites. The increase in CV area is indicative of an increase in charge carrying capacity of the electrode following coating.

Fig. 3. Plots generated from EIS performed before and after coating show decreasing impedance losses with increasing frequency ($n = 92$). (A) Separated real and imaginary impedances show a resistance increase and reactance decrease following coating, with the most pronounced effects occurring at low frequency. (B) The total impedance shows a general decrease with the most pronounced effect also occurring for low frequency. The total impedance is dominated by the imaginary component.

tal probe was not due to surface adhesion of the label directly onto the probe surface. The stability of the coating on the probe was confirmed through continued florescence after inserting the probe into an agarose brain model (data not shown). The coating appeared unaltered after insertion into the model, demonstrating adherence of the coating to the probe given similar mechanical stresses during surgical insertion.

The results of cyclic voltammetry show moderate changes in the voltammogram after coating (Fig. 2A). Larger current magnitudes were found for all voltages along the sweep. Comparing cathodic charge storage capacity before and after coating (Fig. 2B) shows a general increase in charge carrying capacity after coating ($p < 0.001$).

Comparison of the resistance and reactance as a function of frequency show a general increase in resistance and decrease in reactance (Fig. 3A). Comparison of the impedance magnitude before and after coating demonstrates a general decrease in impedance after coating at all frequencies tested (Fig. 3B). Nyquist plots of the electrochemical impedance spectroscopy data show a shift in
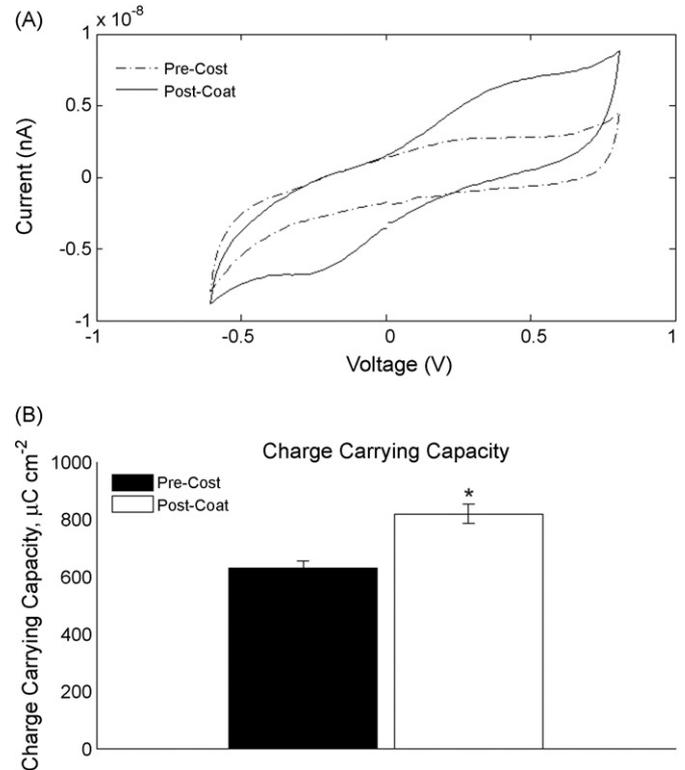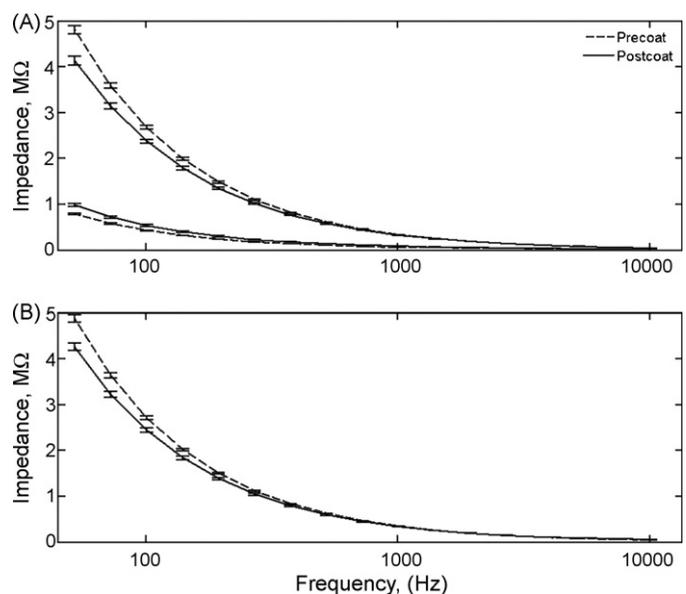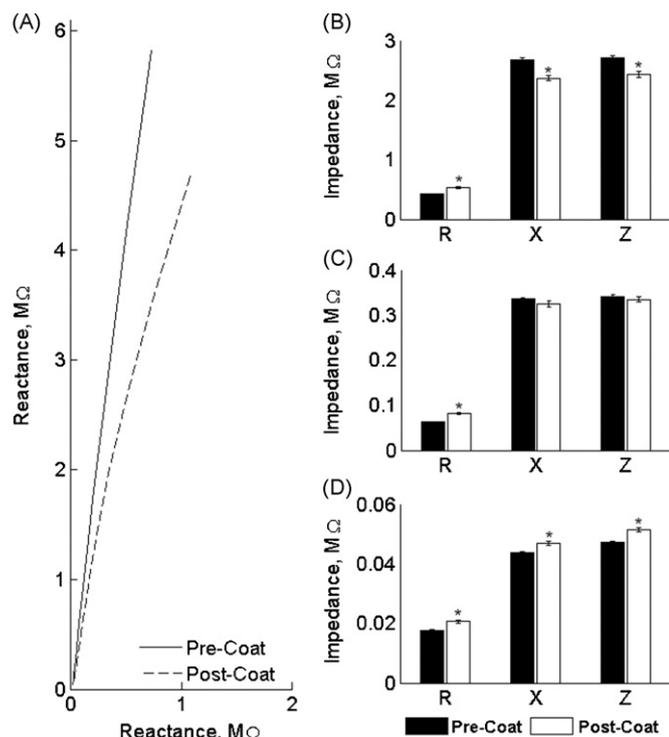
Fig. 4. (A) Representative Nyquist plot generated through electrochemical impedance spectroscopy demonstrates changes in impedance. Spectrograms obtained before and after coating show a moderate decrease in impedance magnitude for all frequencies. (B–D) Bar graphs showing average ($n = 92$) change in resistance (R), reactance (X), and total impedance (Z) following coating for (B) 100 Hz, (C) 1 kHz, and (D) 10 kHz. Resistance increases significantly for all frequencies. Reactance and total impedance decrease significantly at low frequencies, become unchanged near physiological frequencies (*i.e.* 1 kHz), and become significantly higher at high frequencies. The reactance increase at high frequency is much smaller in magnitude than the decrease seen at low frequency.

the impedance curve toward increased resistance and decreased reactance, particularly at low frequencies (Fig. 4A). At low frequencies, both the resistive and reactive changes are more pronounced, with the reactance dominating the total impedance. When the impedances are compared at the individual frequencies of 100 Hz, 1 kHz, and 10 kHz (Fig. 4B–D), the resistance is seen to be significantly increased across all frequencies ($p < 0.001$), whereas the reactance is significantly decreased at 100 Hz ($p < 0.001$), becomes unchanged around 1 kHz ($p = 0.1156$), and is significantly increased at 10 kHz ($p < 0.001$). The 100 Hz decrease is much larger in magnitude than the 10 kHz increase.

4. Discussion

A key consideration in coating an electrode is the manner in which the coating material affects the electrical properties of the probe. Without favorable electrical properties, a coating designed to mitigate the reactive tissue response would be of little value. The results of this study from cyclic voltammetry demonstrate an overall increase in charge carrying capacity for coated electrode sites. Increasing charge carrying capacity corresponds to an increase in sensitivity for recording and allows for higher stimulation currents while minimizing voltage excursions. The increase in charge carrying capacity may be due in part to the decrease in impedance; however, it should be noted that the charge carrying capacity changes may be overestimated since the original site area was used for its calculation, but the porous coating likely increases the surface area across which charge transfer can occur.

The results of EIS show a general decrease in site impedance, with impedance magnitude at the physiologically relevant frequency of 1 kHz being essentially unchanged from a bare electrode. A decrease in site impedance will increase the sensitivity of the electrodes, allowing for the detection of weaker signals and more distant neurons. A decrease in impedance as a result of the application of a non-conductive coating may be a result of increased capacitive charge transfer, and a similar effect following application of thin film coatings has been noted by other investigators (Zhong and Bellamkonda, 2007). The trends seen in the reactance and total impedance support the idea that these impedance decreases are a result of increased capacitance caused by charge separation due to introduction of the layer of thin, nonconductive silica. The impedance for a capacitor is largest at small frequencies and decreases with increasing capacitance. Thus, an increase in capacitance of the electrode interface would account for the reactance trend. In addition, an increase in interfacial capacitance is consistent with the observed increase in charge carrying capacity. The resistance increased for all frequencies, as would be expected for an insulating layer.

The electrical properties of sol–gel produced silica are highly dependent upon the material properties that result from the synthesis and treatment conditions of the film. While thick coatings of sol–gel silica that are sintered and densified by heat treatment substantially increase the total impedance (Hamdy et al., 2007; Pepe et al., 2006), high porosity silica xerogels and aerogels have dielectric constants in the range of 2.1–3.95 (Hong et al., 1997; Kim and Hyun, 2004). Our results demonstrate that the dip-coated, ambient-dried thin film silica sol–gel coatings do not adversely affect the electrical characteristics of the implantable electrodes, and may in fact provide beneficial electrical properties. A major advantage of the sol–gel produced silica is a wide versatility for biofunctionalization. Together these features will allow the sol–gel silica coatings to be used as a platform material for the mitigation of the chronic phase of the reactive tissue response without causing significant detriment to the functionality of the probes.

The modest changes in the electrical properties of the probes should increase signal to noise ratio and improve the quality of neural recordings. However, these effects will likely be small, and the primary benefit of the coating is its use as a platform for biochemical modulation of the electrode tissue interface. The decrease in impedance observed in this study is much smaller than that caused by films or nanotube structures of poly(pyrrole) (PPy) or poly(3,4-ethylenedioxythiophene) (PEDOT), which decrease impedance by two orders of magnitude (Abidian et al., 2006). Likewise, the charge carrying capacity increase is much more subtle than that caused by PPy or PEDOT. Although less advantageous electrically than conductive polymers, sol–gel coatings provide a number of beneficial properties. While polymer nanotubes can deliver only small molecules, sol–gel materials can deliver a wide range of biomolecules. In addition, the rate of release can be finely tuned by adjusting the precursor silane to catalyst ratio (Avnir et al., 2006). Another important point of contrast between silica sol–gel coatings and conducting polymer coatings is the physical scale. While sol–gel coatings have a total thickness of approximately 100 nm, coatings of conductive polymer nanotubes have a thickness ranging from 2 to 8.3 μm (Abidian and Martin, 2008).

The results of this study demonstrate the feasibility of applying silica sol–gel materials to microelectrodes. The potential therapeutic applications that depend on stable chronic recording from the cortex make the mitigation of the reactive tissue response a pressing issue. Silica sol–gels provide an excellent substrate for interaction with neuronal tissue (Jedlicka et al., 2006, 2007a), and thus the ability to successfully coat silicon-based electrodes with this material provides a promising avenue for averting the reactive tissue response.

Acknowledgements

References

Abidian MR, Kim D-H, Martin DC. Conducting-polymer nanotubes for controlled drug release. Advanced Materials 2006;18:405–9.

Abidian MR, Martin DC. Experimental and theoretical characterization of implantable neural microelectrodes modified with conducting polymer nanotubes. Biomaterials 2008;29:1273–83.

Avnir D, Coradin T, Lev O, Livage J. Recent bio-applications of sol–gel materials. Journal of Materials Chemistry 2006;16:1013–30.

Biran R, Martin DC, Tresco PA. Neuronal cell loss accompanies the brain tissue response to chronically implanted silicon microelectrode arrays. Experimental Neurology 2005;195:115–26.

Chen ZJ, Gillies GT, Broaddus WC, Prabhu SS, Fillmore H, Mitchell RM, et al. A realistic brain tissue phantom for intraparenchymal infusion studies. Journal of Neurosurgery 2004;101:314–22.

Cui XY, Lee VA, Raphael Y, Wiler JA, Hetke JF, Anderson DJ, et al. Surface modification of neural recording electrodes with conducting polymer/biomolecule blends. Journal of Biomedical Materials Research 2001;56:261–72.

Cui XY, Martin DC. Electrochemical deposition and characterization of poly(3,4-ethylenedioxythiophene) on neural microelectrode arrays. Sensors and Actuators B-Chemical 2003;89:92–102.

Hamdy AS, Butt DP, Ismail AA. Electrochemical impedance studies of sol–gel based ceramic coatings systems in 3.5% NaCl solution. Electrochimica Acta 2007;52:3310–6.

He W, McConnell GC, Bellamkonda VR. Nanoscale laminin coating modulates cortical scarring response around implanted silicon microelectrode arrays. Journal of Neural Engineering 2006;3:316–26.

Hong J, Yang H, Jo M, Park H, Choi S. Preparation and characterization of porous silica xerogel film for low dielectric application. Thin Solid Films 1997;308–309:495–500.

Jedlicka S, Leavesley SJ, Little KM, Robinson JP, Nivens DE, Rickus JL. Interactions between chemical functionality and nanoscale surface topography impact fibronectin conformation and neuronal differentiation on model sol–gel silica substrates. Materials Research Society Proceedings, Symposium D, Fall Meeting 2006, Boston, MA 2005.

Jedlicka SS, Little KM, Nivens DE, Zemlyanov D, Rickus JL. Peptide ormosils as cellular substrates. Journal of Materials Chemistry 2007a;17:5058–67.

Jedlicka SS, McKenzie JL, Leavesley SJ, Little KM, Webster TJ, Robinson JP, et al. Sol–gel derived materials as substrates for neuronal differentiation: effects of surface features and protein conformation. Journal of Materials Chemistry 2006;16:3221–30.

Jedlicka SS, Rickus JL, Zemyanov DY. Surface analysis by X-ray photoelectron spectroscopy of sol–gel silica modified with covalently bound peptides. Journal of Physical Chemistry B 2007b;111:11850–7.

Johnson MD, Otto KJ, Kipke DR. Repeated voltage biasing improves unit recordings by reducing resistive tissue impedances. IEEE Transactions on Neural Systems and Rehabilitation Engineering 2005;15:160–5.

Kim D-H, Abidian M, Martin DC. Conducting polymers grown in hydrogel scaffolds coated on neural prosthetic devices. Journal of Biomedical Material Research 2004;71A:577–85.

Kim D-H, Martin DC. Sustained release of dexamethasone from hydrophilic matrices using PLGA nanoparticles for neural drug delivery. Biomaterials 2006;27:3031–7.

Kim GS, Hyun SH. Synthesis and characterization of silica aerogel films for inter-metal dielectrics via ambient drying. Thin Solid Films 2004;460:190–200.

Ludwig KA, Uram JD, Yang J, Martin DC, Kipke DR. Chronic neural recordings using silicon microelectrode arrays electrochemically deposited with a poly(3,4-ethylenedioxythiophene) (PEDOT) film. Journal of Neural Engineering 2006;3:59–70.

Moxon KA, Hallman S, Aslani A, Kalkhoran NM, Lelkes PI. Bioactive properties of nanostructured porous silicon for enhancing electrode to neuron interfaces. Journal of Biomaterials Science-Polymer Edition 2007;18:1263–81.

Moxon KA, Kalkhoran NM, Markert M, Sambito MA, McKenzie JL, Webster JT. Nanostructured surface modification of ceramic-based microelectrodes to enhance biocompatibility for a direct brain–machine interface. IEEE Transactions on Biomedical Engineering 2004;51:881–9.

Otto KJ, Johnson MD, Kipke DR. Voltage pulses change neural interface properties and improve unit recordings with chronically implanted microelectrodes. IEEE Transactions on Biomedical Engineering 2006;53:333–40.

Pepe A, Galliano P, Aparicio M, Duran A, Cere S. Sol–gel coatings on carbon steel: electrochemical evaluation. Surface & Coatings Technology 2006;200:3486–91.

Polikov VS, Tresco PA, Reichert WM. Response of brain tissue to chronically implanted neural electrodes. Journal of Neuroscience Methods 2005;148:1–18.

Radin S, Ducheyne P. Controlled release of vancomycin from thin sol–gel films on titanium alloy fracture plate. Biomaterials 2007;28:1721–9.

Radin S, El-Bassyouni G, Vresilovic EJ, Schepers E, Ducheyne P. In vivo tissue response to resorbably silica xerogels as controlled-release materials. Biomaterials 2005;26:1043–52.

Santos EM, Radin S, Ducheyne P. Sol–gel derived carrier for the controlled release of proteins. Biomaterials 1999;20:1695–700.

Spataro L, Dilgen J, Retterer S, Spence AJ, Isaacson M, Turner JN, et al. Dexamethasone treatment reduces astroglia responses to inserted neuroprosthetic devices in rat neocortex. Experimental Neurology 2005;194:289–300.

Szarowski DH, Andersen MD, Retterer S, Spence AJ, Isaacson M, Craighead HG, et al. Brain responses to micro-machined silicon devices. Brain Research 2003;983:23–35.

Vetter RJ, Williams JC, Hetke JF, Nunamaker EA, Kipke DR. Chronic neural recording using silicon-substrate microelectrode arrays implanted in cerebral cortex. IEEE Transactions on Biomedical Engineering 2004;51:896–904.

Wadhwa R, Lagenaur CF, Cui XT. Electrochemically controlled release of dexamethasone from conducting polymer polypyrrole coated electrode. Journal of Controlled Release 2006;110:531–41.

Zhong YH, Bellamkonda RV. Dexamethasone-coated neural probes elicit attenuated inflammatory response and neuronal loss compared to uncoated neural probes. Brain Research 2007;1148:15–27.